Supplemental Materials and Methods

T Cell Repertoire Sequencing and Analysis

For TCR library preparation, we used the commercially available iRepertoire platform (iRepertoire; Huntsville, AL) for nested amplicon arm-PCR (1) of CDR3 regions of the mouse TCR β-chains, with addition of adapters for Illumina platform sequencing. Reverse transcription of 1.5ug of RNA was conducted with the One-Step reverse transcription and amplification kit (Qiagen). The PCR product was purified using Ampure XP magnetic beads (Beckman Coulter), and secondary amplification of the resulting product was performed using GoTaq G2 PCR Kit (Promega), allowing addition of Illumina adapter sequences. Libraries were purified with Ampure XP magnetic beads and sequenced using Illumina MiSeq 250nt paired-end read-length. TCR CDR3 sequences were extracted from the raw sequencing data via the iRmap pipeline (2).

TCR high-throughput sequencing (HTS) data were analyzed in R environment using the tcR package v.2.2.2 (3) and common R routines. TCR repertoire diversity was assessed using True Diversity indices and directly observed richness. Comparative analysis of TCR repertoire richness was performed after normalization of the HTS depth. Total datasets were downsampled to 250,000 randomly chosen sequencing reads using bootstrapping with 1000 iterations. For the comparative analysis of TCR repertoire diversity indices, a downsampling of repertoire sizes to the size of the smallest repertoire was performed using bootstrapping with 1000 iterations. A median of each simulated richness and diversity distribution was used as estimated richness or diversity, accordingly (4). The treatment groups were compared using Kruskal-Wallis ANOVA.

Supplemental References:

1. Han J, et al. Simultaneous amplification and identification of 25 human papillomavirus types with Templex technology. *J Clin Microbiol.* 2006;44(11):4157-62.
2. Wang C, et al. High throughput sequencing reveals a complex pattern of dynamic interrelationships among human T cell subsets. *Proc Natl Acad Sci U S A.* 2010;107(4):1518-23.
3. Nazarov VI, et al. tcR: an R package for T cell receptor repertoire advanced data analysis. *BMC Bioinformatics.* 2015;16:175.
4. Venturi V, Kedzierska K, Turner SJ, Doherty PC, and Davenport MP. Methods for comparing the diversity of samples of the T cell receptor repertoire. *J Immunol Methods.* 2007;321(1-2):182-95.

Supplemental Data

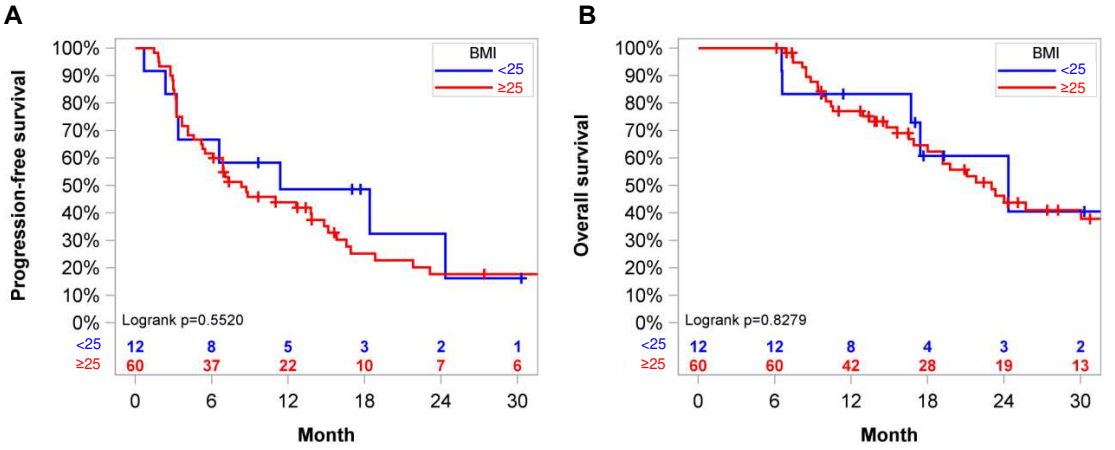

BMI	Median Survival (Month)	6 Month Survival	1 Year Survival	2 Year Survival	Hazard Ratio* (<30 vs ≥30)
<25	11.4	66.7%	48.6%	32.4%	0.84 (0.39, 1.81)
≥25	8.3	61.7%	43.9%	17.7%	P = 0.6622

BMI	Median Survival (Month)	6 Month Survival	1 Year Survival	2 Year Survival	Hazard Ratio* (<30 vs ≥30)
<25	24.3	100%	83.3%	60.8%	0.96 (0.37, 2.54)
≥25	23.0	100%	77.1%	43.8%	P = 0.9406

Supplementary Figure 1. Analysis of metastatic RCC patients with combined overweight or obesity (BMI ≥25kg/m^2) reveals no alteration in PFS or OS, as compared to lean (BMI <25kg/m^2) metastatic RCC patients receiving anti-PD-1. The same patient cohort shown in Figure 1, analyzed for (**A**) Progression-free (PFS) and (**B**) overall survival (OS) of metastatic RCC patients treated withanti-PD-1, categorized by indicated BMI status. Survival curves for PFS and OS across BMI categories were generated with the Kaplan-Meier method. Hazard ratios were calculated from a Cox model controlling for patients' age, sex, IMDC risk score, and number of prior therapies.

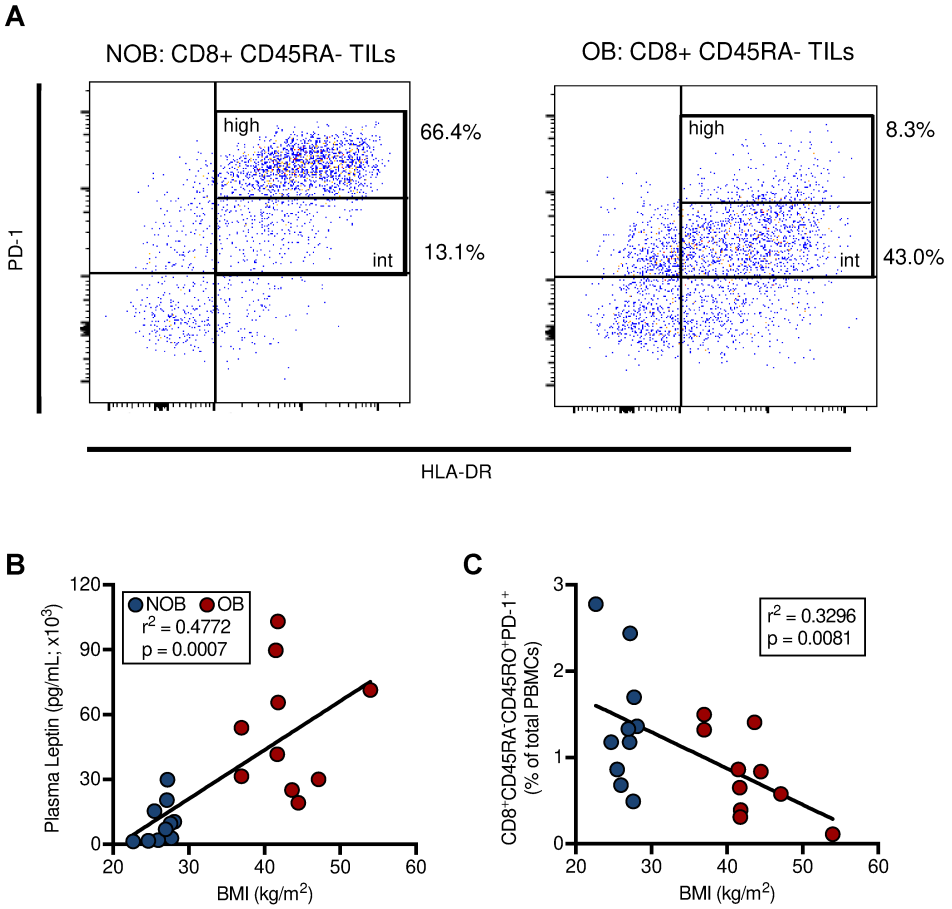

Supplementary Figure 2. BMI differentially correlates with plasma leptin and activated PD-1$^+$ peripheral blood CD8 T cells. (**A**) Representative flow cytometry plots showing PD-1 gating strategy for CD8$^+$CD45RA$^-$ TILs. Linear regression analysis of BMI versus (**B**) plasma leptin or (**C**) peripheral blood activated PD-1$^+$ CD8$^+$ T cells.

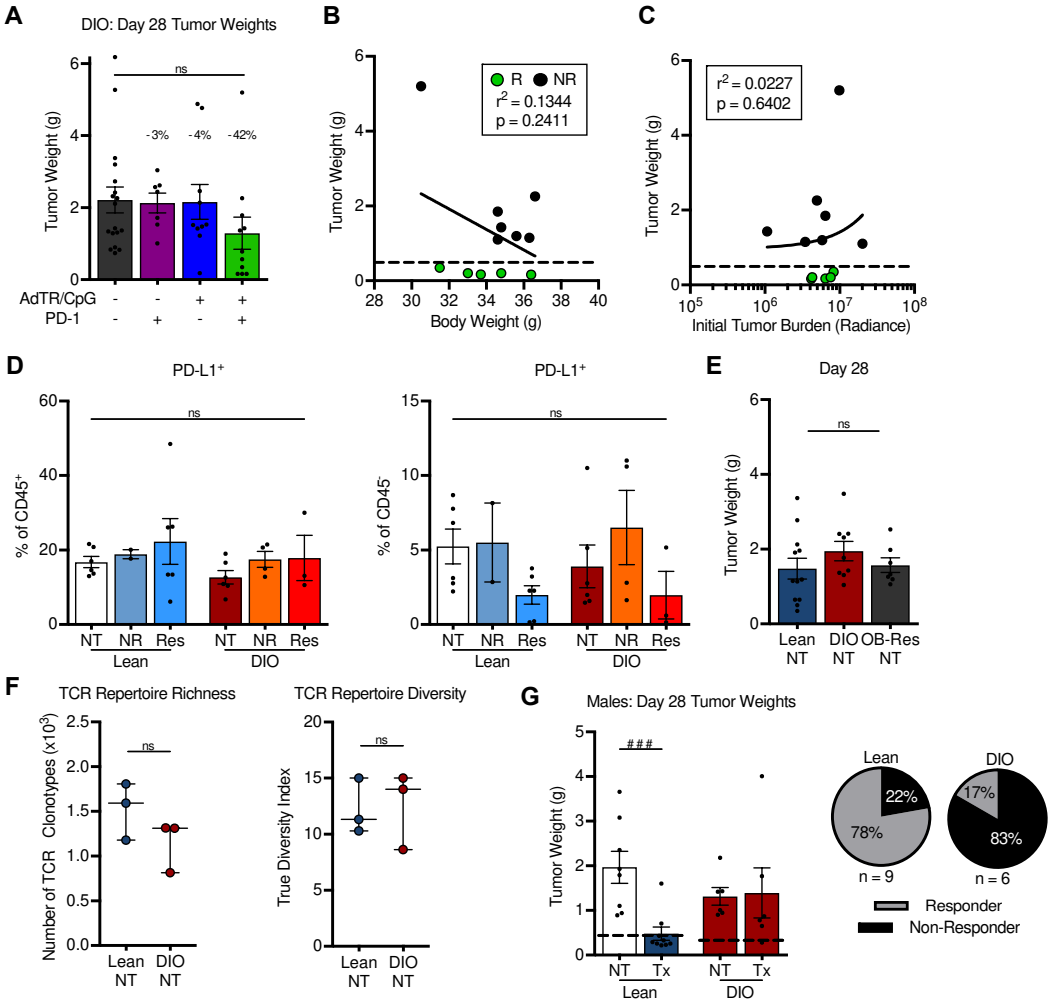

Supplementary Figure 3. Tumor burden at treatment initiation, initial body weight, day 28 PD-L1 expression on intratumoral CD45⁺ and CD45⁻ cells, TCR repertoire and diversity, and sex of mice do not predict or influence treatment outcomes. (**A**) Day 28 tumor weights for DIO animals treated with NT, single agent anti-PD-1, AdTR/CpG, or AdTR/CpG/PD-1. Regression analysis between day 28 tumor weights and (**B**) initial body weight at tumor challenge or (**C**) initial tumor burden at the time of treatment initiation on day 7. Responders (R) = green and non-responders (NR) = black. (**D**) Percentages of PD-L1⁺ cells at day 28 among (left) CD45⁺ and (right) CD45⁻ cells. (**E**) Day 28 tumor weights of NT Lean, DIO, and OB-Res mice (repeated data from Fig. 3F). (**F**) Whole-tumor TCRβ CDR3 sequencing analysis from day 28 excised tumors. High throughput sequencing reads-normalized repertoire (left) richness and (right) diversity. (**G**) Day 28 renal tumor weights for lean and DIO male mice, treated as previously indicated, and resulting AdTR/CpG/PD-1 response rates. (**B-E,G**) Data are pooled from at least two independent experiments or (**A,F**) a single experiment and presented as means ± SEM. Statistical differences were determined using non-parametric Mann-Whitney U tests (###p<0.001), linear regression analyses, or two-way ANOVA. NT = no therapy; NR = non-responder; Res = responder; Tx = AdTR/CpG/PD-1.

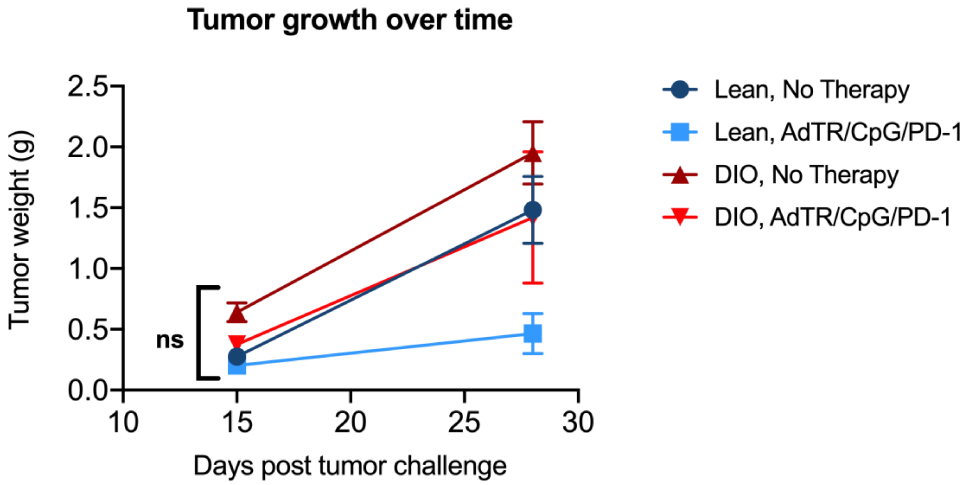

Day 28 Comparisons	Significance	Adjusted p-value
Lean, No Therapy vs. Lean, AdTR/CpG/PD-1	**	0.0041
Lean, No Therapy vs. DIO, No Therapy	ns	0.9240
Lean, No Therapy vs. DIO, AdTR/CpG/PD-1	ns	>0.9999
Lean, AdTR/CpG/PD-1 vs. DIO, No Therapy	****	<0.0001
Lean, AdTR/CpG/PD-1 vs. DIO, AdTR/CpG/PD-1	*	0.0191
DIO, No Therapy vs. DIO, AdTR/CpG/PD-1	ns	0.7813

Supplemental Figure 4. Mixed-effects modeling of tumor growth over time confirms loss of therapeutic efficacy in DIO mice with orthotopic renal tumors as compared to lean counterparts. Mixed-effects model with Bonferroni correction analysis was completed on cumulative data of day 15 and day 28 post tumor-challenge tumor weights in no therapy and AdTR/CpG/PD-1-treated lean and DIO mice. No significant differences were detected at day 15 post-tumor challenge. Differences detected at day 28 post-tumor challenge are detailed in the table above.

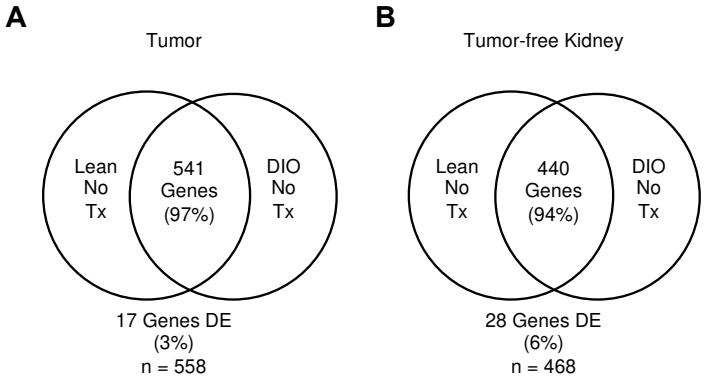

Supplementary Figure 5. The immunogenetic landscape of intratumoral and tumor-free kidneys is minimally altered by obesity in the absence of immunotherapy. Tumor samples and contralateral tumor-free kidneys from lean and DIO treatment-naive mice were collected at day 28 post-tumor challenge and analyzed using nanoString's PanCancer Immune Profiling platform. (**A**) Analysis of differentially expressed (DE) genes within tumors indicates equivalent gene expression in 97% of genes examined. (**B**) Analysis of DE genes in tumor-free kidneys indicates equivalent gene expression in 94% of genes examined. Data are from one experiment. Tx = AdTR/CpG/PD-1.

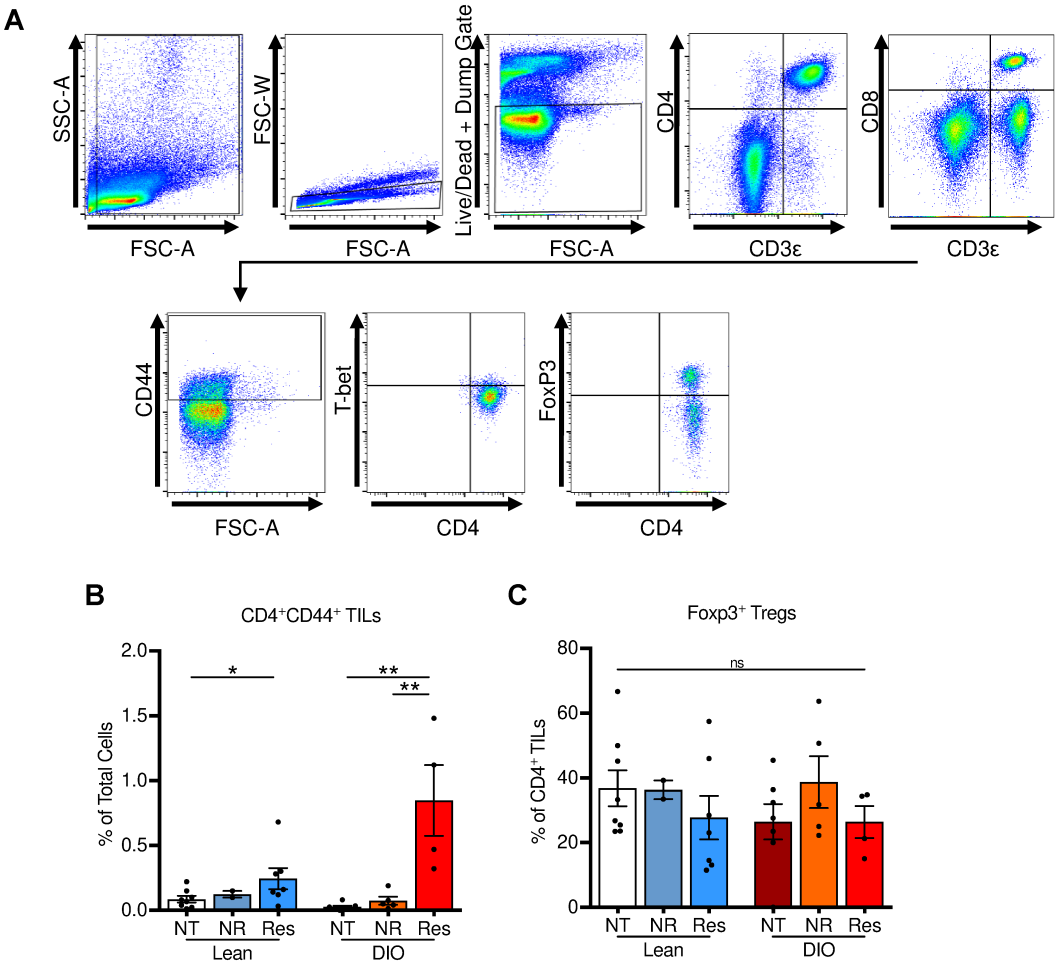

Supplementary Figure 6. Intratumoral CD4⁺ T cell populations from lean and DIO mice. On day 28 post tumor challenge, intratumoral T cells were analyzed by flow cytometry. (**A**) Gating strategies used and resulting frequencies of (**B**) activated CD4⁺ TILs and (**C**) CD4⁺Foxp3⁺ Tregs. Data are presented as means ± SEM from at least two independent experiments. Statistical differences were determined using two-way ANOVA followed by post hoc Bonferroni's multiple comparisons tests (*p<0.05, **p<0.01, ***p<0.001). NT = no therapy; NR = non-responder; Res = responder.

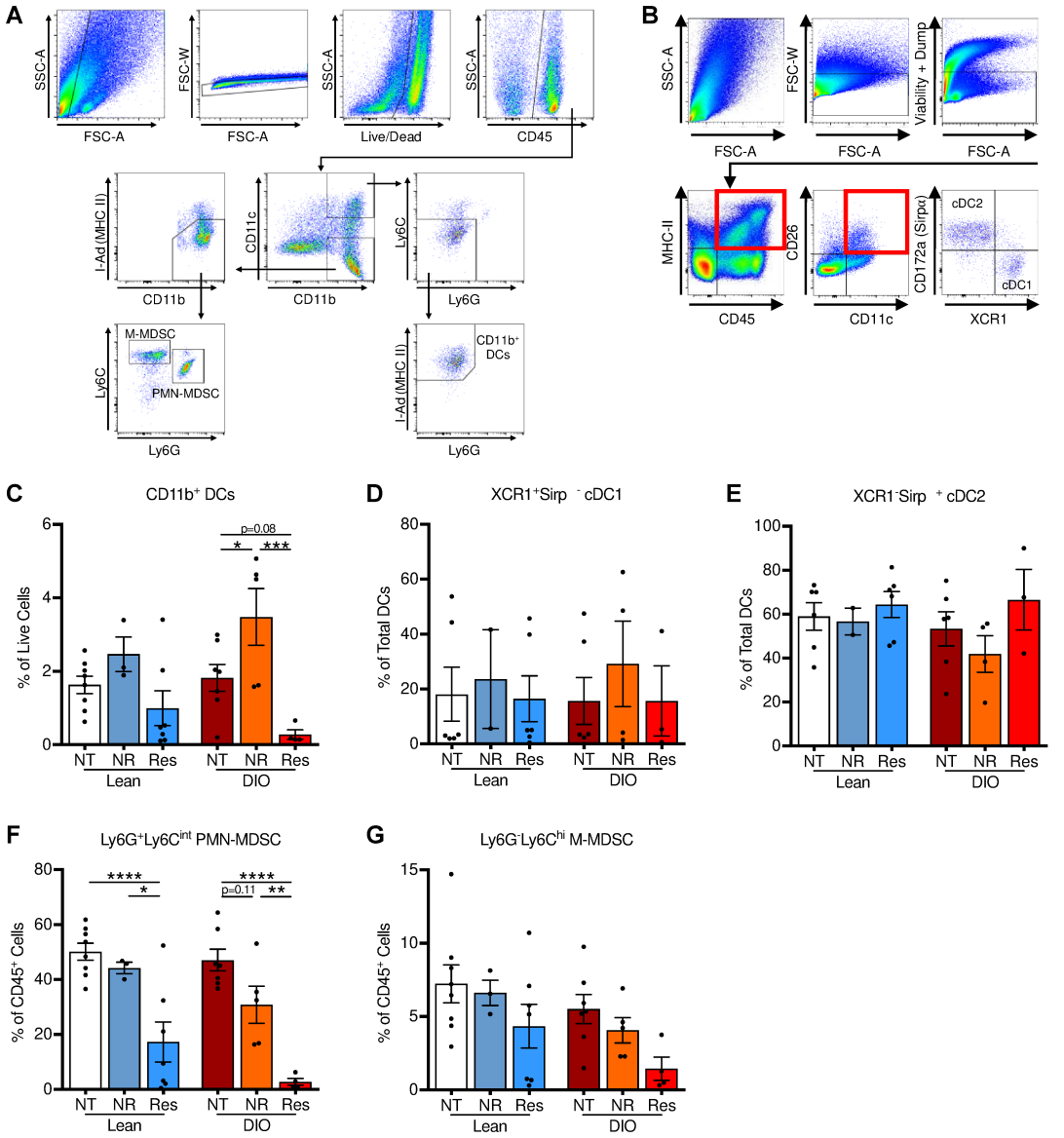

Supplementary Figure 7. Intratumoral MDSC and DC populations in lean and DIO mice. On day 28 post-tumor challenge, intratumoral MDSCs and DCs from lean and DIO mice receiving no therapy or AdTR/CpG/PD-1 were analyzed by flow cytometry. (**A,B**) Gating strategies and resulting frequencies of (**C**) CD11b$^+$ DCs, (**D**) XCR1$^+$Sirp**α**$^-$ cDC1s, (**E**) XCR1$^-$ Sirp**α**$^+$ cDC2s, (**F**) Ly6G$^+$Ly6C^{int} polymorphonuclear (PMN) MDSCs, and (**G**) Ly6G$^-$Ly6C^{hi} monocytic (M) MDSCs. Data are presented as means ± SEM from at least two independent experiments. Statistical differences were determined using two-way ANOVA followed by post hoc Bonferroni's multiple comparisons tests (*p<0.05, **p<0.01, ***p<0.001, ****p<0.0001). NT = no therapy; NR = non-responder; Res = responder.

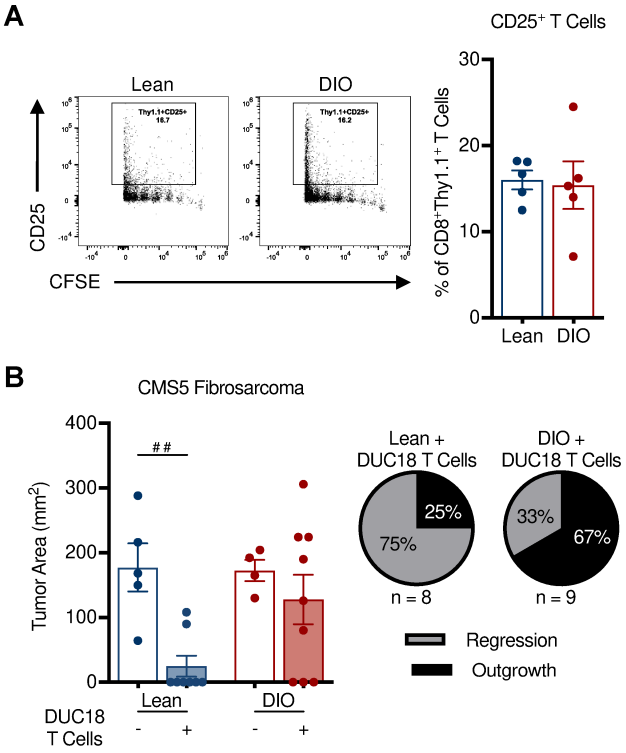

Supplementary Figure 8. In mice with transplanted fibrosarcoma, the obese host environment does not hinder upstream T cell priming, but T cell-mediated tumor clearance remains impaired. Lean and DIO BALB/c mice were challenged with subcutaneous CMS5 fibrosarcoma. On day 4 post tumor challenge, antigen-specific DUC18 T cells were adoptively transferred into a subset of mice while others remained as no-transfer controls. Four days after adoptive transfer with CFSE-labeled DUC18 T cells, tumor-draining lymph nodes were harvested from a subset of animals and stained for (**A**) CFSE and CD25 on DUC18 Thy1.1⁺CD8⁺ T cells. (**B**) Endpoint tumor areas at day 21 for DUC18 T cell recipients or day 15 for no-transfer controls. Pie charts indicate percentages of DUC18 recipients with tumor outgrowth or regression. Data are pooled from at least two independent experiments and presented as means ± SEM. Statistical differences were calculated using non-parametric Mann-Whitney U tests (##p<0.01).

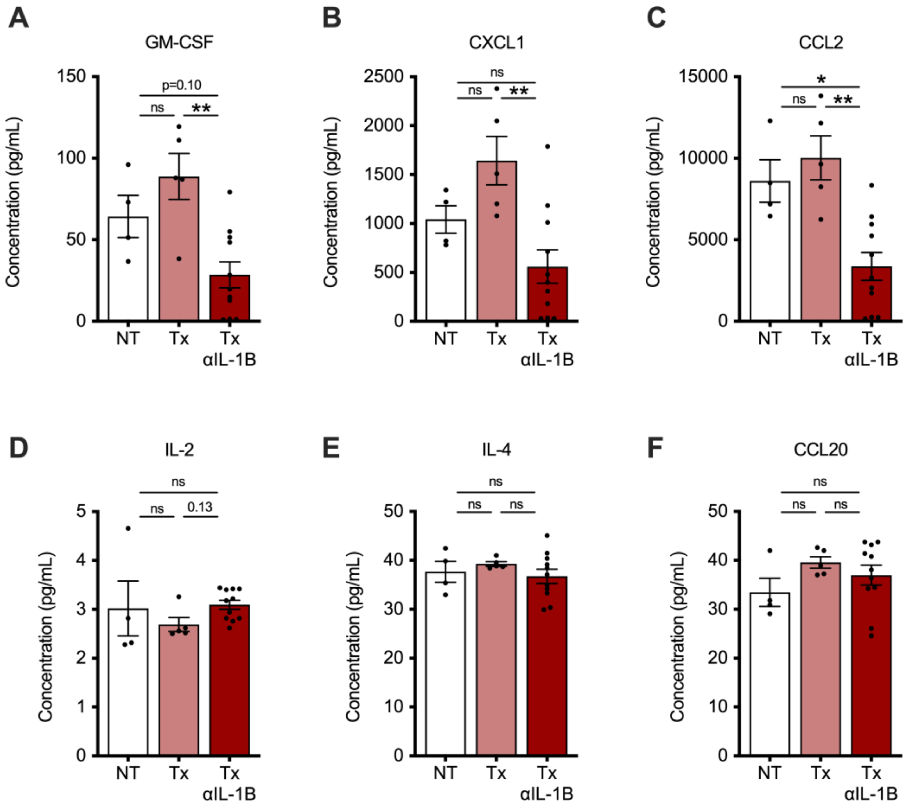

Supplementary Figure 9. Neutralization of IL-1B results in the specific reduction in the concentration of multiple myeloid-associated cytokines/chemokines in the obese renal tumor microenvironment but has little to no off-target effects on unrelated cytokines. DIO animals were treated with no therapy or AdTR/CpG/PD-1 ± anti-IL-1β neutralizing antibody. Day 28 endpoint quantification of the intratumoral concentrations of myeloid-related (A) GM-CSF, (B) CXCL1, and (C) CCL2. Data are pooled from two independent experiments and presented as means ± SEM. Statistical differences were calculated using parametric one-way ANOVA (*p<0.05, **p<0.01). Intratumoral concentrations of unrelated (D) IL-2, (E) IL-4, and (F) CCL20 were assessed for any potential any off-target effects of neutralization. Data are pooled from two independent experiments and presented as means ± SEM. Statistical differences were calculated using either parametric one-way ANOVA or non-parametric Kruskal Wallis ANOVA. NT = no therapy and Tx = AdTR/CpG/PD-1 therapy.

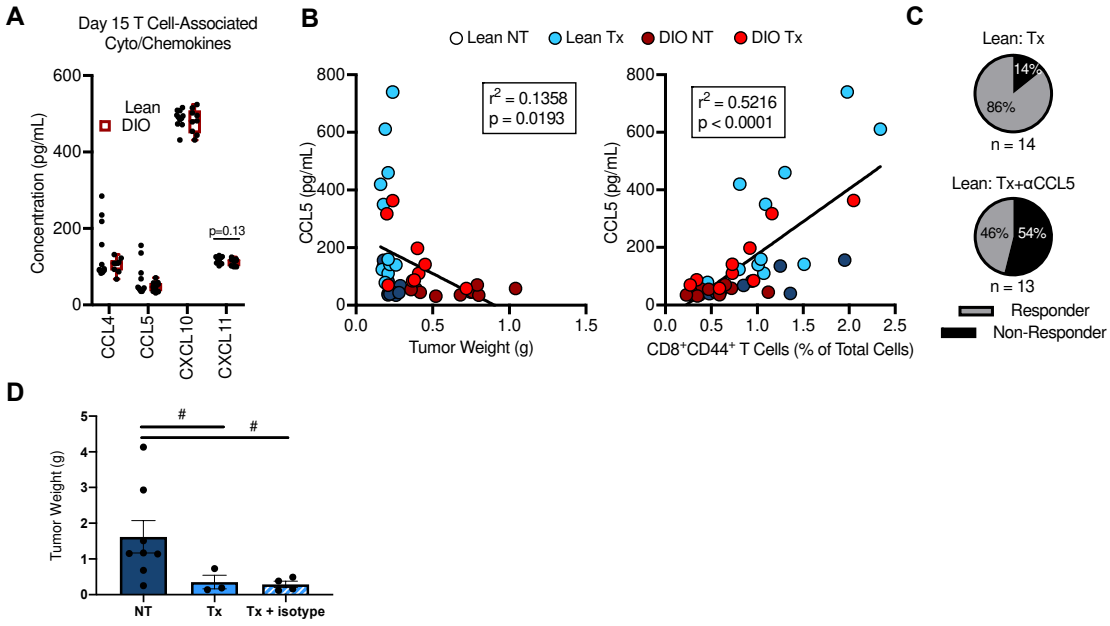

Supplementary Figure 10. CCL5 neutralization impairs immunotherapy response in lean mice. On day 15 post tumor challenge lean and DIO treatment-naive mice were evaluated for (**A**) intratumoral T cell-associated cyto/chemokines. (**B**) Linear regression of intratumoral CCL5 concentrations versus (left) tumor weight and (right) associated leukocyte populations in lean and DIO therapy-naive and therapy-treated animals. (**C**) Day 28 response rates for lean animals receiving AdTR/CpG/PD-1 ± anti-CCL5 neutralizing antibody. **(D)** Day 28 comparison of lean mice receiving no therapy or AdTR/CpG/PD-1 ± isotype control. Isotype administration had no effect on therapeutic efficacy. Data are pooled from at least two independent experiments and presented as means ± SEM. Statistical differences were calculated using parametric t-tests, non-parametric Mann-Whitney U tests, linear regression analyses, or Kruskal-Wallis ANOVA as appropriate. NT = no therapy and Tx = AdTR/CpG/PD-1 therapy.

Supplemental Table 1. Demographics and characteristics of anti-PD-1 treated RCC patients.

	BMI at 1st dose < 30							BMI at 1st dose ≥ 30							
Variable	N	Mean	SD	Median	Min	Max	Frequency (%)	N	Mean	SD	Median	Min	Max	Frequency (%)	p value*
Age	43	66.4	8.9	66.5	43	86		29	66.4	9.6	65.0	47.0	81.0		0.8277
Male	43						31 (72.1%)	29						22 (75.9%)	0.7219
Race	43							29							1.0000
White							38 (88.4%)							26 (89.7%)	
AA							4 (9.3%)							2 (6.9%)	
Other							1 (2.3%)							1 (3.5%)	
Ethnic group	43							29							1.0000
Non-Hispanic/Latino							42 (97.7%)							28 (96.5%)	
Unknown							1 (2.3%)							1 (3.5%)	
Smoker	27							16							1.0000
Yes							14 (51.9%)							9 (56.3%)	
No							13 (48.1%)							7 (43.7%)	
BMI at time of 1st dose	43	26.5	2.7	27.1	20.7	29.4		29	36.2	5.1	34.3	30.3	48.8		<0.0001
Latest BMI	43	25.7	3.9	26.5	18.2	32.4		29	35.6	6.1	34.7	25.7	50.7		<0.0001
Diff of BMI (1st - latest)	43	0.9	2.7	0.2	-4.3	6.7		29	0.6	4.4	0.6	-11.9	7.4		0.7924
Follow up time (days)	43	638.8	316.5	585	187	1212		29	506.3	273.4	422.0	211.0	1269.0		0.0958
Number of doses of nivolumab	43	17.9	15.0	11.0	3.0	60		28	15.2	15.2	8.5	3.0	72.0		0.2635
Treatment duration (days)	41	302.5	287.5	196	28	1139		27	242.1	259.6	148.0	33.0	1269.0		0.4073
Histological subtype	43							29							
Clear cell							37 (86.0%)							24 (82.8%)	0.7015
Papillary							4 (9.3%)							2 (6.9%)	
Unclassified							2 (4.7%)							3 (10.3%)	
IMDC risk score	42							29							0.7266
0							13 (31.0%)							8 (27.6%)	
1							16 (38.1%)							11 (37.9%)	
2							12 (28.6%)							7 (24.1%)	
3							1 (2.4%)							2 (6.9%)	
4							0							1 (3.5%)	
Number of prior treatments	43							29							0.2785
0							3 (7.0%)							1 (3.5%)	
1							24 (55.8%)							20 (69.0%)	
2							12 (27.9%)							5 (17.2%)	
3							4 (9.3%)							1 (3.5%)	
4							0							2 (6.9%)	
Autoimmune Hypothyroidism	41							28							0.6415
Yes							3 (7.3%)							1 (3.6%)	
No							39 (92.9%)							27 (96.4%)	
Deceased	43						18 (41.9%)	29						18 (62.1%)	0.0926
Best response	43							29							0.7613
SD							20 (46.5%)							15 (51.7%)	
PD							13 (30.2%)							9 (31.0%)	
PR							5 (11.6%)							1 (3.5%)	
CR							1 (2.3%)							1 (3.5%)	

OR present, not measured							1 (2.3%)								2 (6.9%)	
Stopped for toxicity, death, or unknown							3 (7.0%)								1 (3.5%)	
Objective response rate (ORR)	43						7 (16.3%)		29						4 (13.8%)	1.0000
Disease control rate (DCR)	43						27 (62.8%)		29						19 (65.5%)	0.8132
*** Wilcoxon test for continuous variables and Fisher's exact test for categorical variables**																

2

14

Supplemental Table 2. Demographics and characteristics of treatment-naive renal cancer subjects used for TIL analysis.

	Renal Cancer Subjects	
	NOB	OB
Subjects (n)	8	11
Sex	M 75.00% F 25.00%	M 45.50% F 54.50%
Age (years, mean)	63.38	58.27
Age (years, range)	42 – 77	46 – 71
BMI (kg/m^2, mean)	25.02	42.24
BMI (kg/m^2, range)	19.80 – 28.49	30.66 – 62.78
Histologic Subtype		
Clear Cell	100.00%	73.00%
Other	0.00%	27.00%
Stage (%)		
T1a	12.50%	36.36%
T1b	25.00%	36.36%
T2a	12.50%	9.09%
T2b	12.50%	0.00%
T3a	37.50%	9.09%
T3b	0.00%	0.00%
N/A	0.00%	9.09%
Grade		
1	0.00%	0.00%
2	50.00%	54.55%
3	25.00%	27.27%
4	25.00%	0.00%
NA	0.00%	18.18%

Supplemental Table 3. Demographics and characteristics of treatment-naive renal cancer subjects and tumor-free donors used for peripheral blood analysis.

	Renal Cancer Subjects		Tumor-Free Subjects	
	NOB	OB	NOB	OB
Subjects (n)	37	45	11	8
Sex	M 70.27% F 29.73%	M 57.78% F 42.22%	M 27.27% F 72.73%	M 50.00% F 50.00%
Age (years, mean)	59.00	57.44	60.64	54.63
Age (years, range)	28 – 83	41 – 81	35 – 76	48 – 68
Weight (kg, mean)	76.34	118.42	72.67	100.05
BMI (kg/m^2, mean)	25.07	38.74	25.16	32.58
BMI (kg/m^2, range)	18.24 – 29.98	30.00 – 60.73	21.52 – 29.45	30.10 – 38.60
Diabetes (%)	13.51%	37.78%	Unavailable	Unavailable
Histologic Subtype				
Clear Cell	84.00%	89.00%		
Other	16.00%	11.00%		
Stage (%)				
T1a	54.05%	35.56%		
T1b	13.51%	35.56%		
T2a	2.70%	4.44%		
T2b	2.70%	2.22%		
T3a	24.32%	20.00%		
T3b	2.70%	0.00%		
N/A	0.00%	2.22%		
Grade				
1	0.00%	4.44%		
2	32.43%	55.56%		
3	45.95%	20%		
4	16.22%	11.11%		
NA	5.41%	8.89%		

Supplemental Table 4. Differentially expressed (DE) genes shared between Lean R vs NR and DIO R vs NR which overlap with yellow, blue, and green clusters from Figure 5A.

Yellow Cluster Overlap (79 genes)

Abcb1a	*Cd200*	*Cd8a*	*Cxcl12*	*Gpi1*	*Il17f*	*Ltb*	*Rps6*
Adora2a	*Cd34*	*Cd8b1*	*Cxcl14*	*Gzma*	*Il6st*	*Map3k5*	*Sigirr*
Angpt1	*Cd36*	*Cdh1*	*Cxcl16*	*H2-Aa*	*Irf1*	*Mavs*	*Syt17*
App	*Cd3e*	*Ceacam1*	*Cxcr3*	*H2-Ab1*	*Irf3*	*Nrp1*	*Tek*
C8a	*Cd3g*	*Cfb*	*Cxcr6*	*H2-DMb2*	*Irf8*	*Nt5e*	*Thbd*
C8g	*Cd55*	*Chuk*	*Dock9*	*Icam1*	*Itga6*	*Pml*	*Thy1*
Ccl19	*Cd59b*	*Cmpk2*	*Dpp4*	*Icam2*	*Jam3*	*Prf1*	*Tie1*
Ccl21a	*Cd6*	*Ctsh*	*Dusp6*	*Ifit3*	*Kit*	*Psen1*	*Tnfsf10*
Ccl27a	*Cd74*	*Cx3cl1*	*Ecsit*	*Il15*	*Klrc1*	*Psen2*	*Xbp1*
Ccl5	*Cd79b*	*Cxcl11*	*F2rl1*	*Il16*	*Klrd1*	*Rorc*	

Blue Cluster Overlap (96 genes)

Amica1	*Ccl12*	*Cd84*	*Cxcl2*	*Il17rb*	*Itga5*	*Nup107*	*Tgfb1*
Atf1	*Ccl2*	*Cd97*	*Cxcr2*	*Il18*	*Itgam*	*Oas2*	*Thbs1*
Bcl10	*Ccl24*	*Cdk1*	*Dusp4*	*Il18r1*	*Itgb1*	*Osm*	*Tlr4*
Bcl2	*Ccl3*	*Cfp*	*F13a1*	*Il18rap*	*Jak3*	*Ptgs2*	*Tlr5*
Bcl6	*Ccl7*	*Clec4a2*	*Fcer1g*	*Il1b*	*Lcn2*	*Pvr*	*Tnfrsf10b*
Btk	*Ccr1*	*Clec4n*	*Fcgr1*	*Il1r1*	*Litaf*	*Rel*	*Tnfrsf1b*
C3ar1	*Cd163*	*Clec5a*	*Fos*	*Il1r2*	*Ly96*	*Runx1*	*Tnfsf18*
C4b	*Cd200r1*	*Creb5*	*Gpr183*	*Il1rl1*	*Lyve1*	*Serpinb2*	*Trem1*
C5ar1	*Cd244*	*Csf2rb*	*H60a*	*Il1rn*	*Lyz2*	*Siglec1*	*Trem2*
C6	*Cd33*	*Csf3r*	*Hif1a*	*Il4ra*	*Msr1*	*Slc7a11*	*Ulbp1*
Card9	*Cd37*	*Ctsl*	*Ifitm2*	*Il6*	*Mx2*	*Socs3*	*Usp18*
Casp1	*Cd68*	*Cxcl1*	*Il13ra2*	*Il6ra*	*Nlrp3*	*Tank*	*Vhl*

Green Cluster Overlap (42 genes)

Anxa1	*Ccl8*	*Chil3*	*Ifi35*	*Lgals3*	*Oasl1*	*Spn*
Arg1	*Ccl9*	*Csf2*	*Ifngr1*	*Masp1*	*Plaur*	*Tal1*
Birc5	*Cd40*	*Cxcl3*	*Il12rb1*	*Mst1r*	*S100a8*	*Tnfrsf12a*
Bst1	*Cd47*	*H2-M3*	*Irak4*	*Myc*	*Serping1*	*Tnfrsf13c*
C1s1	*Cdkn1a*	*Hspb2*	*Isg15*	*Ncf4*	*Smn1*	*Tnfrsf9*
Ccl6	*Cebpb*	*Ifi27*	*Lbp*	*Oas3*	*Snai1*	*Vim*

Supplemental Table 5. List of antibodies and dyes used in this study.

***In Vivo* Antibodies**				
Antigen	**Clone**	**Fluorochrome**	**Catalog number**	**Supplier**
PD-1 (CD279)	RMP1-14	none	BE0146	BioXCell
Rat IgG2a Isotype Control	2A3	none	BE0089	BioXCell
IL-1B	B122	none	BE0246	BioXCell
CCL5	53405	none	MAB478	R&D Systems
Dyes for Flow Cytometry				
Dye	**Clone**	**Fluorochrome**	**Catalog number**	**Supplier**
CFSE	N/A	N/A	C34570	ThermoFisher
Zombie Aqua Viability Dye	N/A	N/A	423102	BioLegend
Zombie Green Viability Dye	N/A	N/A	423111	BioLegend
Murine Antibodies for Flow Cytometry				
Antigen	**Clone**	**Fluorochrome**	**Catalog number**	**Supplier**
CD3ε	145-2C11	APC, FITC	100312, 100305	BioLegend
CD4	GK1.5	APC/Fire750	100460	BioLegend
CD8α	53-6.7	PE/Cy7, A488, APC	100722, 100723, 100712	BioLegend
CD11b	M1/70	BV510, PE/Cy7	101263, 101216	BioLegend
CD11c	N418	BV510, APC/Cy7	117338, 117324	BioLegend
CD19	6D5	FITC	115505	BioLegend
CD25	PC61	BV421	102033	BioLegend
CD26	H194-112	PE	137803	BioLegend
CD44	IM7	PerCP-Cy5.5	103032	BioLegend
CD45	30-F11	Pacific Blue, PerCP-Cy5.5	103126, 103132	BioLegend
CD45R (B220)	RA3-6B2	FITC	103205	BioLegend
CD64	X54-5/7.1	FITC	139315	BioLegend
CD90.1 (Thy1.1)	HIS51	APC	170900-82	eBioscience
CD161	PK136	FITC	108705	BioLegend
CD172a (Sirpα)	P84	PE-Dazzle 594	144016	BioLegend
CD274 (PD-L1)	10F.9G2	BV605	124321	BioLegend
CD279 (PD-1)	29F.1A12	BV421, APC/Fire750	135218, 135240	BioLegend
F4/80	BM8	FITC	123107	BioLegend
Foxp3	150D	A647	320014	BioLegend
I-A/I-E (MHC II)	M5/114.15.2	BV650	107641	BioLegend
I-A^d (MHC II)	39-10-8	Alexa Fluor 488	115008	BioLegend
IFNγ	XMG1.2	BV421	505830	BioLegend
Ly6C	HK1.4	BV605	128036	BioLegend
Ly6G	1A8	PerCP-Cy5.5	127615	BioLegend
Perforin	S16009A	PE	154306	BioLegend
TNFa	MP6-XT22	PE/Cy7	506324	BioLegend
XCR1	ZET	BV421	148216	BioLegend
Human Antibodies for Flow Cytometry				
Antigen	**Clone**	**Fluorochrome**	**Catalog number**	**Supplier**
CD3	HIT3a	PE	300308	BioLegend
CD8	HIT8a	PerCP-Cy5.5	300924	BioLegend
CD45RA	HI100	BV421	304130	BioLegend
CD45RO	UCHL1	FITC	35-0457-T100	TONBO Biosci.
CD279 (PD-1)	EH12.2H7	PE/Cy7	329918	BioLegend
HLA-DR	L243	APC/Cy7	307618	BioLegend